

The Meta Distribution of the SIR for Cellular Networks with Power Control

Yuanjie Wang, Martin Haenggi, and Zhenhui Tan

Abstract

The *meta distribution* of the signal-to-interference ratio (SIR) provides fine-grained information about the performance of individual links in a wireless network. This paper focuses on the analysis of the meta distribution of the SIR for both the cellular network uplink and downlink with fractional power control. For the uplink scenario, an approximation of the interfering user point process with a non-homogeneous Poisson point process is used. The moments of the meta distribution for both scenarios are calculated. Some bounds, the analytical expression, the mean local delay, and the beta approximation of the meta distribution are provided. The results give interesting insights into the effect of the power control in both the uplink and downlink. Detailed simulations show that the approximations made in the analysis are well justified.

Index Terms

Stochastic geometry, Poisson point process, Cellular network, SIR, Uplink, Downlink, Power control

I. INTRODUCTION

A. Motivation and the meta distribution

The meta distribution (of the SIR) has been proposed in [1], where it is applied to both Poisson bipolar networks and downlink cellular networks without power control to answer the questions

Yuanjie Wang and Zhenhui Tan are with the State Key Laboratory of Railway Traffic Control and Safety, Beijing Jiaotong University, Beijing, 100044, China (e-mail: wang.yuanjie@outlook.com). Martin Haenggi is with the Dept. of Electrical Engineering, University of Notre Dame, IN, 46556, USA (e-mail: mhaenggi@nd.edu). The work was supported by National Natural Science Foundation of China (61471030) and the US National Science Foundation (grant CCF 1525904). Revision Date: February 8, 2017.

such as “What fraction of users in a network can achieve a desired link reliability given the required SIR threshold?” or “How is the success probability of individual links distributed in each network realization?” Such questions are often asked by network operators and indeed of great significance for providing guidance to the practical deployment of the wireless networks. However, these questions have not been answered analytically for the uplink in cellular networks. The uplink, compared to its downlink counterpart, is more complex in the network structure and requires power control to maintain the link quality and mitigate the inter-cell interference. These differences make the analysis of uplink in the framework of the meta distribution more challenging. Meanwhile, since the meta distribution provides more fine-grained information including the variance of the conditional success probability and the mean local delay, etc., an examination of the effect of power control in the downlink is also warranted.

Formally, the meta distribution of the SIR in cellular network is defined as

$$\bar{F}(\theta, x) \triangleq \bar{F}_{P_s}(\theta, x) = \mathbb{P}^o(P_s(\theta) > x), \quad \theta \in \mathbb{R}^+, x \in [0, 1], \quad (1)$$

where $P_s(\theta) \triangleq \mathbb{P}(\text{SIR} > \theta \mid \Phi)$ is the conditional success probability averaged over the fading and the random activities of the interferers given the point process, \mathbb{P}^o denotes the Palm measure of the point process, given an active receiver at the origin, and the SIR is measured at that receiver.

For the meta distribution, $P_s(\theta)$ can be interpreted as the reliability, *i.e.*, the success probability of the link in consideration given the SIR threshold θ . The meta distribution corresponds to the fraction of links in each network realization that achieve an SIR of θ with reliability at least x .

The b -th moment of $P_s(\theta)$ (with regard to the Palm measure) is defined as

$$M_b(\theta) \triangleq \mathbb{E}^o(P_s(\theta)^b), \quad b \in \mathbb{C}. \quad (2)$$

By this definition and noting that the random variable $P_s(\theta) \in [0, 1]$, we have

$$M_b(\theta) = \int_0^1 x^b dF_{P_s}(x) \stackrel{(a)}{=} \int_0^1 bx^{b-1} \bar{F}_{P_s}(x) dx,$$

with (a) following integration by parts, and we easily obtain $p_s(\theta) \equiv M_1(\theta)$, *i.e.*, the first moment

of the conditional success probability is the standard success probability, as expected.

B. Related work

In the analysis of wireless networks with randomly deployed nodes based on stochastic geometry theory, the Poisson point process (PPP) is the most widely used model due to its analytical tractability. The tractability of PPP is a consequence of the independence between the points, which is formally captured by Slivnyak's theorem [2]. It also results in a simple expression for the probability generating functional (PGFL) [2]. Most of the existing studies focus on some performance metric as a function of the SIR at the typical receiver in the network obtained by averaging over the channel fading and the point process by utilizing the Laplace transform of the interference, which is obtained from the PGFL. However, such a spatial average only yields limited information about the individual links. In particular, the success probability $p_s(\theta) \triangleq \mathbb{P}(\text{SIR} > \theta)$ is one of the most important performance metric of interest, usually being interpreted as the probability that the typical receiver can achieve a target SIR threshold. Informally, in stochastic geometry, this "typical point" (the typical receiver) originates from a selection procedure in which every point of the point process must have the same chance of being selected, hence, the success probability is in fact a result of *spatial averaging* over the entire point process. It can only quantify the overall SIR performance of the network, but provides no detailed statistical information for the performance of each individual link in the network. To obtain fine-grained information on the SIR and reveal how the success probabilities are distributed among the individual links, the meta distribution of the SIR has been formally proposed in [1]. The concept of the conditional success probability dates back to [3], where it is used to study the local delay in ad hoc networks modeled by PPPs. In [1] the meta distribution is applied to study Poisson bipolar networks with ALOHA channel access and the downlink of Poisson cellular networks, and closed-form expressions of the b -th moment of the conditional success probability for the two network classes are derived. In [4] the conditional success probability is used to study Poisson bipolar networks without a channel access scheme. The asymptotic behavior of the distribution is studied and the moments are calculated. In [5] the meta distribution is analyzed

for the scenario of D2D communication underlaid with the downlink of Poisson cellular networks with ALOHA channel access, and the moments of the conditional SIR distribution, the mean local delay of both the typical D2D receiver and the typical cellular receiver are derived.

For Poisson cellular networks with the nearest-BS association criterion but no power control, the downlink is easy to model and analyze since the interfering BSs to the typical receiver form a PPP conditioned on the distance to the serving BS, and, without power control, the aggregate interference experienced by the typical receiver has no relation with the link distances within the interfering cells. Furthermore, the average interfering signal power from each interfering BS is by definition smaller than the average signal power from the serving BS, which simplifies the derivations. These advantages make the downlink cellular network model thoroughly studied [6]–[10] and easier to be combined with many types of emerging techniques, *e.g.*, cooperative transmission [11]–[13], MIMO [14]–[16], and D2D communication [17]–[19].

The uplink case is quite different: on the one hand, the interfering user in a neighboring cell can be much closer to a BS than the transmitting user in the cell of that BS; on the other hand, the interfering user point process seen at the typical BS is not a PPP and hard to model due to the correlation between the Voronoi cells of the *Poisson-Voronoi tessellation* and the channel access scheme in each cell. Moreover, due to the different distance ratios between the desired and interfering links compared to the downlink, it can be expected that power control at the user leads to improved performance in the uplink.

For the uplink, various models have been proposed to approximate the network performance. [20] analyzes the coverage performance in K -tier uplink Poisson cellular networks with truncated channel inversion power control, but the model used there is ill-defined, since the user model is generated from an assumed PPP with “sufficiently high density” to make the network fully loaded, *i.e.*, to have an active user in each cell. Also the approximation of the interfering user point process by a homogeneous PPP is inaccurate. [21] studies the uplink SIR distributions in a two-tier heterogeneous cellular network by considering the effect of a multi-level power control scheme and approximating the interferer locations of a tier as a non-uniform Poisson point process, whose intensity at a location x is the intensity of the BSs in that tier multiplied

by a probability factor that if there was a point of the active user process at x , it would belong to the Voronoi cell of another BS (of the same tier) rather than the reference one. A similar non-uniform PPP approximation with the intensity multiplied by a probability factor is also used in [22] and [23] by conditioning on a user at the origin to analyze the full-load case (*i.e.*, all BSs are active), but the approximation model is questionable. Firstly, the probability factor is interpreted as the probability that a user is deemed interfering, however, in their user model, which has only one active user per channel per cell, an active user is definitely interfering as long as it is not at the origin; moreover, conditioning on a given user at the origin but performing spatial averaging over all users means that the user resides in the *Crofton cell* [24], which makes that user not typical among the active users in the network. [25] models the interfering user point process as a homogeneous PPP excluding the ball centered at the analyzed BS with the radius determined through matching the average number of excluded points from that homogeneous PPP and the non-homogeneous PPP in [22]. Again, they rely on the assumption of a PPP with “sufficiently high density”, which is impractical and not rigorous. Recently, [26] defines the point process of active users rigorously and provides a non-homogeneous PPP approximation based on the pair correlation function of the interfering user point process from the typical BS point of view. This approximation is significantly more accurate than the one in [22] and [23].

C. Contributions

The paper makes the following contributions:

- We derive analytical expressions of the b -th moment for the Poisson cellular networks with fractional power control for both uplink and downlink and calculate the analytical meta distribution of the SIR for the two scenarios.
- We investigate the effect of the fractional power control on the mean local delay, which is the -1-st moment of the conditional success probability.
- We show that the meta distribution of the SIR for both the uplink and downlink Poisson cellular networks can be accurately approximated by the beta distribution through matching the first and second moments.

- We reveal the trade-off between the first moment of the conditional success probability and its variance and discuss the optimal operating range of the power control parameter.

II. META DISTRIBUTION FOR THE UPLINK

A. Network model

We consider a single-tier uplink Poisson cellular network of type I in [26], where base stations (BSs) are modeled as $\Phi_b = \Phi \cup \{o\}$, where $\Phi \subset \mathbb{R}^2$ is a homogeneous PPP with intensity λ . By Slivnyak's theorem, the BS at the origin becomes the typical BS under expectation over Φ_b . The spectrum resources are channelized, and each BS is assumed to schedule only one user on each channel. For a given channel, each user is uniformly distributed in the Voronoi cell of the serving BS. Formally, the user point process is defined as $\Phi_u \triangleq \{y \in \Phi_b : U(V(y))\}$, where $V(y)$ denotes the Voronoi cell of BS y ; $U(B)$, $B \subset \mathbb{R}^2$, denotes a point chosen uniformly and randomly from B , and independently across different B .

The network model is depicted in Fig. 1. The user served by the typical BS is the typical user, and its location is denoted by x_0 . The distance from each user x to its own serving BS is denoted by R_x ; for the typical user, the subscript x_0 is omitted, so $R = \|x_0\|$. We denote the interfering user point process as Φ_I , given by $\Phi_I = \Phi_u \setminus \{x_0\}$. The distance from the interfering user located at x to the typical BS is denoted by $D_x = \|x\|$. The standard power-law path loss model with exponent $\alpha > 2$ for signal propagation and the standard Rayleigh fading are used. In this case, the power fading coefficients h_x associated with the user at x and the typical BS are exponentially distributed variables with unit mean, *i.e.*, $h_x \sim \exp(1)$. We assume $\{h_x\}$ are independent for all $x \in \Phi_u$.

We use the fractional power control at the user in the form $P_x = pR_x^{\alpha\epsilon}$, which is one of the most widely used schemes for the uplink cellular networks. The power control exponent $\epsilon \in [0, 1]$ is introduced to partially compensate for the path loss, p is the baseline transmit power when there is no power control. Noise is neglected, *i.e.*, an interference-limited scenario is considered.

We shall note that the model used here and the models used by the previous work [20], [22], [23], [25] are similar but have important differences. The previous work also considers the

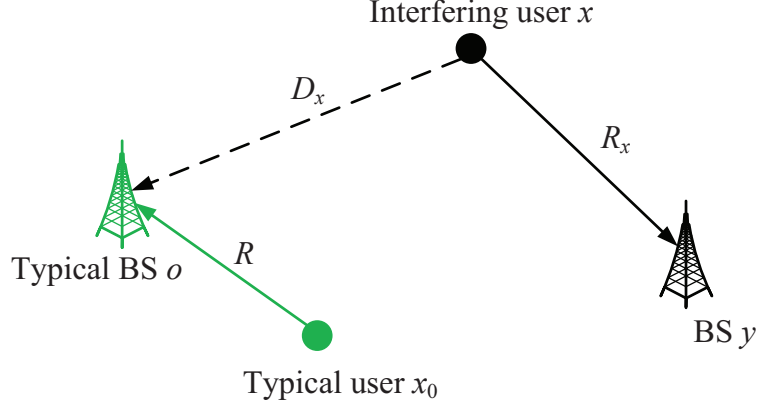


Fig. 1. Uplink network model. The typical BS is at the origin, the typical user served by it is x_0 .

full-load uplink scenario and single-user scheduling on each channel. However, their definition of the network model is in accordance with the type II model in [26], while their analysis is performed on the type I model. As we have explained in Sec. I-B, they are actually analyzing the performance of a user in the Crofton cell, which means their “typical user” is not, in fact, the typical active user.

For our network setup, the uplink SIR at the typical BS is given by

$$\text{SIR} \triangleq \frac{P_{x_0} h_{x_0} R^{-\alpha}}{\sum_{x \in \Phi_I} P_x h_x D_x^{-\alpha}}.$$

For the typical user, $P_{x_0} = pR^{\alpha\epsilon}$, thus

$$\text{SIR} = \frac{h_{x_0} R^{\alpha(\epsilon-1)}}{\sum_{x \in \Phi_I} R_x^{\alpha\epsilon} h_x D_x^{-\alpha}}. \quad (3)$$

To analyze the SIR performance, we need to know the statistical properties of Φ_I and the distribution of the link distances in the network.

B. PPP Approximation of Φ_I

Since $o \in \Phi_b$ and the typical user is not an interferer, Φ_I is a non-stationary process whose intensity depends on the distance from the origin. Its exact statistics are hopeless to derive, but

[26] provides an accurate approximation of its intensity function, given by

$$\lambda_I(x) = \lambda \left(1 - \exp \left((-12/5) \lambda \pi \|x\|^2 \right) \right). \quad (4)$$

A non-homogeneous PPP with this intensity function can then be used to approximate Φ_I , as suggested in [26].

Remark 1: The earlier work [22] and [23] on the uplink scenario approximates Φ_I by a non-homogeneous PPP with intensity

$$\lambda_I(x) = \lambda (1 - \exp(-\lambda \pi \|x\|^2)), \quad (5)$$

with the factor $1 - \exp(-\lambda \pi \|x\|^2)$ being interpreted as the probability that a user at the point x is interfering to the typical BS at the origin. But as we have indicated in Sec. I-B, this is not accurate, since a user not served by the reference BS, wherever it is located, is for sure an interferer, so this probability is 1, trivially. Moreover, such an approximation does not take the pair correlation between points in Φ_I into account, hence it is only a crude approximation. We can verify this by inspecting Ripley's K function in Fig. 2. It clearly shows that the approximation (5) for the uplink interfering user point process underestimates the number of the interferers in the proximity of the BS (e.g., in the range of r from 0.4 to 1), yielding an underestimation of the average aggregate interference suffered by the typical BS, while the approximation (4) closely matches the simulation result. We can also see that the interfering user point process outside a large enough radius of the typical BS approaches the PPP asymptotically and the new approximation (4) also slightly underestimates the K function, but this has negligible effect on the interference as the signal power decays quickly with the distance.

C. Distribution of the Link Distances

For the SIR model in (3), we use a Rayleigh distribution to characterize the link distance distribution according to the method used in [26] with the probability density function (pdf)

$$f_R(r) = \frac{5}{2} \pi \lambda r \exp \left(-\frac{5}{4} \lambda \pi r^2 \right), \quad r \geq 0, \quad (6)$$

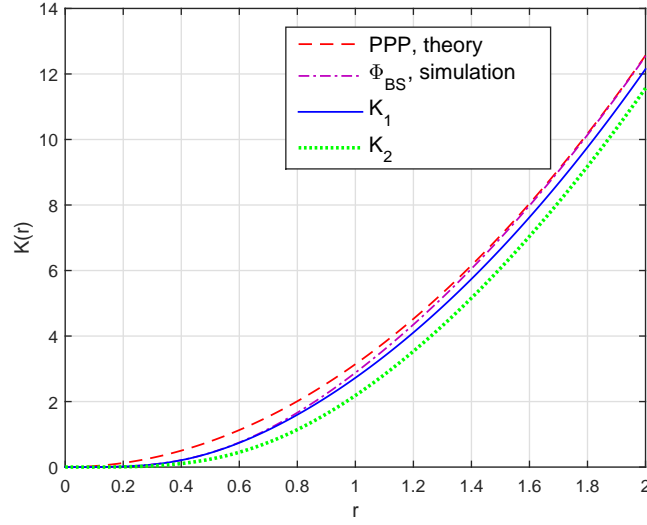


Fig. 2. Ripley's K function. $K_1(r) = \pi r^2 + 5/12e^{-12/5\pi r^2} - 5/12$ corresponds to (5) in [26] and $K_2(r) = \pi r^2 + e^{-\pi r^2} - 1$ is K function of the interfering user point process approximated by the non-homogeneous PPP in [22] and [23]. Both the Ripley's K functions of the standard PPP in theory and that of the interfering user point process at the typical BS by simulation are shown for comparison.

which is obtained by matching the mean of the Rayleigh distribution with the empirical mean from simulation. Compared to the link distance in the Crofton cell (F_1 in Fig. 3), there is a factor $5/4$ in this pdf. R_x should have the same distribution as R , however, noting that R_x cannot be larger than D_x , we characterize the distribution of R_x by conditioning on D_x to capture the dependency. This results in the truncated Rayleigh distribution

$$f_{R_x}(r|D_x) = \frac{(5/2)\pi\lambda r \exp(-(5/4)\lambda\pi r^2)}{1 - \exp(-(5/4)\lambda\pi D_x^2)}, \quad 0 \leq r \leq D_x. \quad (7)$$

This truncation partially captures the correlation between R_x and D_x that is present for x near the origin.

Remark 2: The earlier work [22], [23] uses the Rayleigh distribution for the distribution of the link distance R and a truncated version of the same Rayleigh distribution for the interfering link distances $\{R_x\}$, $x \in \Phi_I$ conditioned on the fact $R_x \leq D_x$,

$$f_R(r) = 2\pi\lambda r \exp(-\lambda\pi r^2), \quad r \geq 0, \quad (8)$$

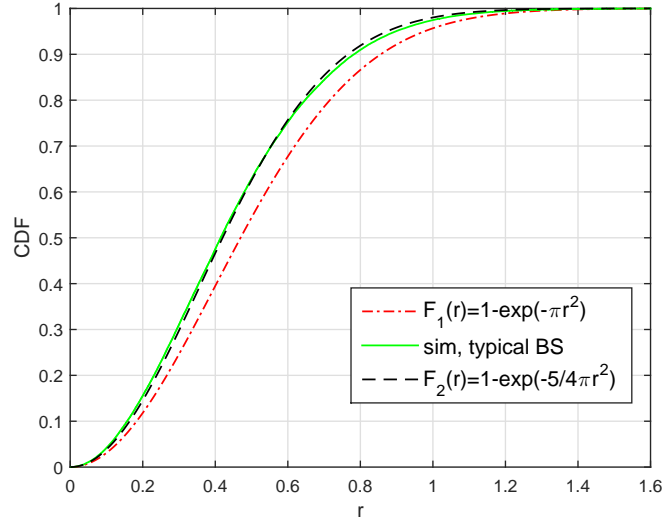


Fig. 3. Link distance distribution comparison. $F_1(r)$ corresponds to the pdf in (8), $F_2(r)$ corresponds to the pdf in (6), both for $\lambda = 1$.

$$f_{R_x}(r|D_x) = \frac{2\pi\lambda r \exp(-\lambda\pi r^2)}{1 - \exp(-\lambda\pi D_x^2)}, \quad 0 \leq r \leq D_x. \quad (9)$$

However, this does not match the uplink network model in use, since (8) is obtained by conditioning on a user at the origin and treating R as the contact distance. So R and $\{R_x\}$ are not identically distributed due to the difference between the Crofton cell and the typical cell, as we have discussed in Sec. II-B. Fig. 3 shows that (8) deviates significantly from the actual link distance distribution obtained from the simulation.

Equipped with (4), (6) and (7), we can derive an approximation of the b -th moment of $P_s(\theta)$.

D. Moments

Theorem 1 (Moments of $P_s(\theta)$ for uplink Poisson cellular networks) *The b -th moment M_b of the conditional success probability of the uplink Poisson cellular networks with FPC under the non-homogeneous PPP approximation (4) for the interfering user point process is closely approximated by*

$$\tilde{M}_b = \int_0^\infty \exp\left(-z \left(1 + \int_0^\infty f_b(z, x) dx\right)\right) dz, \quad (10)$$

where $f_b(z, x) = \int_0^x B_1^{-1} z e^{-zy} \frac{1 - e^{-zx B_2/B_1}}{1 - e^{-zx}} \left(1 - (1 + \theta y^{\frac{\alpha\epsilon}{2}} x^{-\frac{\alpha}{2}})^{-b}\right) dy$, $B_1 = 1.25$, $B_2 = 12/5$, $\alpha > 2$ and $\epsilon \in [0, 1]$.

Proof: The conditional coverage probability is

$$\begin{aligned} P_s(\theta) &= \mathbb{P}\left(h_{x_0} > \theta \sum_{x \in \Phi_I} h_x D_x^{-\alpha} R_x^{\alpha\epsilon} R^{\alpha(1-\epsilon)} \mid \Phi_a, \Phi_b\right) \\ &= \prod_{x \in \Phi_I} \frac{1}{1 + \theta \left(\frac{R^{(1-\epsilon)} R_x^{\epsilon}}{D_x}\right)^{\alpha}}. \end{aligned} \quad (11)$$

Then M_b follows as

$$\begin{aligned} M_b &= \mathbb{E} \prod_{x \in \Phi_I} \frac{1}{\left(1 + \theta \frac{R^{\alpha(1-\epsilon)} R_x^{\alpha\epsilon}}{D_x^{\alpha}}\right)^b} \\ &= \mathbb{E} \prod_{x \in \Phi_I} \mathbb{E}_{R_x} \left(\frac{1}{\left(1 + \theta \frac{R^{\alpha(1-\epsilon)} R_x^{\alpha\epsilon}}{D_x^{\alpha}}\right)^b} \mid D_x, R \right) \\ &\stackrel{(a)}{\approx} \mathbb{E} \prod_{x \in \Phi_I} \int_0^{D_x} \frac{(5/2)\pi \lambda x e^{-(5/4)\lambda \pi x^2}}{1 - e^{-(5/4)\lambda \pi D_x^2}} \frac{1}{(1 + \theta x^{\alpha\epsilon} D_x^{-\alpha} R^{\alpha(1-\epsilon)})^b} dx \\ &\stackrel{(b)}{=} \mathbb{E}_R \exp \left(\int_0^\infty -2\lambda \pi \left(1 - e^{-B_2 \lambda \pi a^2}\right) \right. \\ &\quad \cdot \left. \left(1 - \int_0^a \frac{(5/2)\pi \lambda x e^{-(5/4)\lambda \pi x^2}}{1 - e^{-(5/4)\lambda \pi a^2}} \frac{1}{(1 + \theta x^{\alpha\epsilon} a^{-\alpha} R^{\alpha(1-\epsilon)})^b} dx \right) da \right) \\ &\stackrel{(c)}{=} \int_0^\infty (5/2)\pi \lambda r \exp \left(\int_0^\infty -2\lambda \pi \left(1 - e^{-B_2 \lambda \pi a^2}\right) \left(1 - \int_0^a \frac{(5/2)\pi \lambda x e^{-(5/4)\lambda \pi x^2}}{1 - e^{-(5/4)\lambda \pi a^2}} \frac{1}{(1 + \theta x^{\alpha\epsilon} a^{-\alpha} r^{\alpha(1-\epsilon)})^b} dx \right) da \right) e^{-(5/4)\lambda \pi r^2} dr, \end{aligned} \quad (12)$$

where (a) uses (7) to average over R_x ; (b) follows from (4) and the PGFL of the general PPP [2], which is given by

$$\mathbb{E} \prod_{x \in \Phi} f(x) = \exp \left(- \int_{\mathbb{R}^2} [1 - f(x)] \Lambda(dx) \right);$$

(c) uses (6) to average over R .

Then by using substitution $\frac{x}{r} = u$, $\frac{r}{a} = v$ and $e^{-\lambda \pi r^2} = t$, after some simplification, we obtain

$M_b \approx \tilde{M}_b$, with \tilde{M}_b given in (10). ■

Corollary 1 (Special case: $\epsilon = 1$) When $\epsilon = 1$,

$$\tilde{M}_b = \exp \left(\frac{1}{B_1} \int_0^1 \int_0^1 \frac{1 - u^{B_2/B_1}}{1 - u} (A - u^{x-1} h(x)) \, du dx \right), \quad (13)$$

where $B_1 = 5/4$, $B_2 = 12/5$, $A = 1 - (1 + \theta)^{-b}$, $h(x) = \frac{b\theta\alpha x^{\alpha/2-1}}{2(1+\theta x^{\alpha/2})^{b+1}}$.

Proof: By substituting $z = \ln t$ and $\epsilon = 1$ into (10), after some simplification, we obtain \tilde{M}_b in the form

$$\tilde{M}_b = \int_0^1 t^{g(t)} dt, \quad (14)$$

where

$$g(t) = \int_0^\infty \int_0^s -\frac{1}{B_1} \frac{1 - t^{sB_2/B_1}}{1 - t^s} \ln t \cdot t^y \left(1 - (1 + \theta y^{\frac{\alpha}{2}} s^{-\frac{\alpha}{2}})^{-b} \right) dy ds. \quad (15)$$

$g(t)$ can be expressed as

$$\begin{aligned} g(t) &\stackrel{(a)}{=} -\ln t \int_0^\infty \frac{1}{B_1} \frac{1 - t^{sB_2/B_1}}{1 - t^s} \int_0^1 st^{sx} \left(1 - \frac{1}{(1 + \theta x^{\frac{\alpha}{2}})^b} \right) dx ds \\ &\stackrel{(b)}{=} -\int_0^\infty \frac{1}{B_1} \frac{1 - t^{sB_2/B_1}}{1 - t^s} \left(\int_0^1 (At^s - t^{sx} h(x)) dx \right) ds \\ &\stackrel{(c)}{=} \frac{1}{B_1} \log_t e \int_0^1 \int_0^1 \frac{1 - u^{B_2/B_1}}{1 - u} (A - u^{x-1} h(x)) du dx, \end{aligned} \quad (16)$$

where (a) follows from the substitution $y/s = x$; (b) from integration by parts; (c) from replacing t^s with u . Finally, by insterting $g(t)$ into (14) we obtain (13). ■

Fig. 4 shows the standard success probability $p_s = M_1$ and the variance of the conditional success probability as a function of θ for $\alpha = 4$ and FPC parameter $\epsilon = 0, 0.5, 1$. The solid and dashed curves correspond to the simulation results, the markers correspond to the analytical results in Theorem 1. These results reveal how the FPC parameter affects M_1 and the variance. For the low-SIR regime, a higher ϵ benefits both M_1 and the variance, which means it improves the average performance of the network and also reduces the difference between the individual links, resulting in better fairness. Conversely, a higher FPC exponent ϵ harms the average

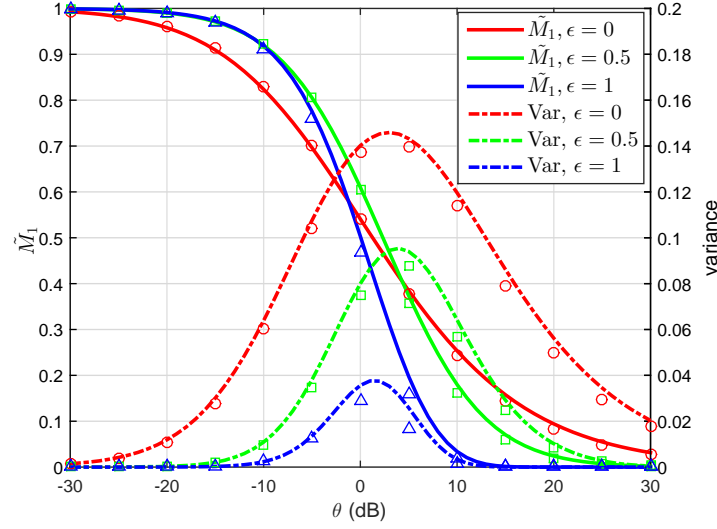


Fig. 4. The first moment and variance of $P_s(\theta)$ in the uplink for different ϵ , $\alpha = 4$. The curves are the analytical \tilde{M}_1 and variance from Theorem 1 (*i.e.*, $\text{Var} = \tilde{M}_2 - \tilde{M}_1^2$); the markers correspond to the simulated M_1 and variance.

performance of the network in the high-SIR regime, because for large θ , assuming no power control, only users very close to their BSs will succeed. However, with power control, these users have to drastically reduce their transmit powers relative to the interferers, which reduces the received signal strength at their BSs and thus the SIR. Hence, they are increasingly less likely to succeed as ϵ grows. The users far away from their BSs are unlikely to benefit from the path loss compensation due to the high SIR threshold. As a result, the average network performance is brought down.

Fig. 4 also shows the significance of the meta distribution as a much more refined metric than just M_1 . For example, if the target SIR is -3 dB, all values of ϵ lead to a very similar M_1 , so M_1 alone does not tell us which ϵ to use, but if we consider the variance, it is evident that $\epsilon = 1$ is best.

Theoretically, ϵ can be greater than 1, which is the over-compensation case. The analytical results are shown in Fig. 5 and Fig. 6. It is shown that generally speaking, over-compensation of the transmit power has no benefit to the network, especially for the high-SIR threshold regime, this is because raising the transmit power too much makes the receiver more likely to experience

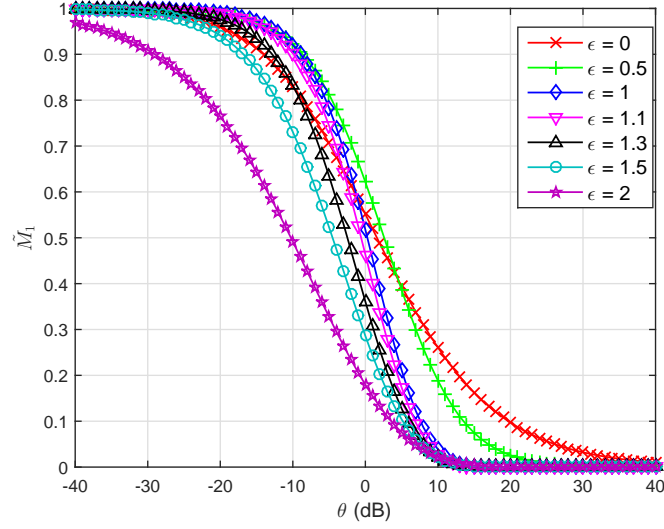


Fig. 5. Uplink \tilde{M}_1 obtained from (10) for different values of ϵ and $\alpha = 4$.

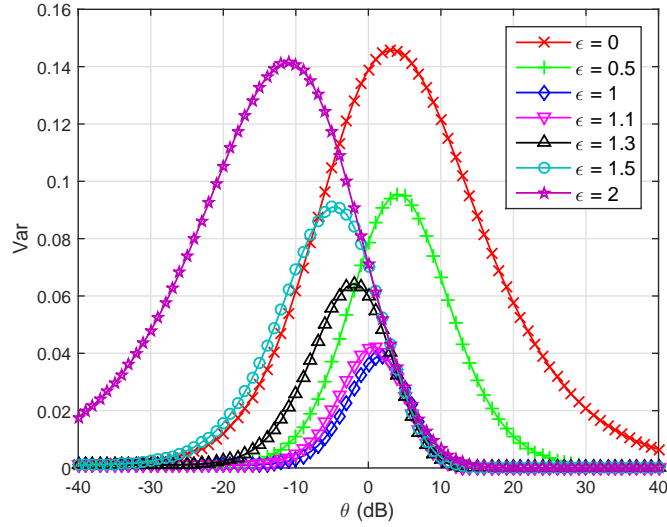


Fig. 6. Variance of $P_s(\theta)$ obtained from (10) for different values of ϵ and $\alpha = 4$ in the uplink.

interference from transmitters far away, and the incremental interference power dominates the increment of the useful signal power.

Corollary 2 (Asymptotic property of ϵ) Define $\epsilon_{\text{opt}}^{(1)}(\theta) = \arg \max_{\epsilon} \tilde{M}_1(\theta)$, $\theta \in \mathbb{R}^+$. Then we

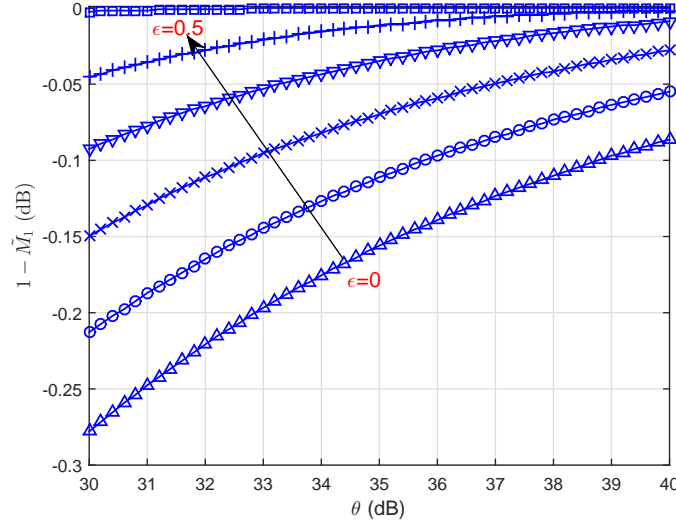


Fig. 7. The asymptotic property of uplink \tilde{M}_1 when $\theta \rightarrow \infty$. $\epsilon = 0, 0.1, 0.2, 0.3, 0.4, 0.5$ from bottom to top.

have $\lim_{\theta \rightarrow \infty} \epsilon_{\text{opt}}^{(1)}(\theta) = 0$.

Proof: By observing the structure of the expression (10) for $b = 1$, since the exponential function is monotonically increasing, and the integration interval is the positive real axis, it is easy to see that to maximize \tilde{M}_1 , $-1 - \int_0^\infty f_1(z, x) dx$ should reach the maximum. Then the integrand $f_1(z, x) = \int_0^x z e^{-zy} \left(1 - (1 + \theta y^{\epsilon\alpha/2} x^{-\alpha/2})^{-1}\right) dy$ should take the minimum since it is always positive. For the integrand of $f_1(z, x)$, the factor e^{-zy} is monotonically decreasing for $y \in (0, x)$, while the factor $1 - (1 + \theta y^{\epsilon\alpha/2} x^{-\alpha/2})^{-1} = \frac{y^{\epsilon\alpha/2} x^{-\alpha/2}}{\theta^{-1} + y^{\epsilon\alpha/2} x^{-\alpha/2}}$, which is monotonically increasing for $y \in (0, x)$, when $\theta \rightarrow \infty$, $\frac{y^{\epsilon\alpha/2} x^{-\alpha/2}}{\theta^{-1} + y^{\epsilon\alpha/2} x^{-\alpha/2}}$ will approach 1, the dominant term is e^{-zy} . Thus the integral is minimized at $\epsilon = 0$. ■

Fig. 7 illustrates the result in Cor. 2. It can be seen that as θ increases, the $1 - \tilde{M}_1$ (in dB) for $\epsilon = 0$ is always below the curves for the other values of ϵ , which means that for large enough θ , \tilde{M}_1 is maximized at $\epsilon = 0$.

M_{-1} is the *mean local delay* that quantifies the mean number of transmission attempts needed before the first success if the transmitter is allowed to keep transmitting [27]. According to [1], the mean local delay of downlink Poisson cellular networks without power control experiences

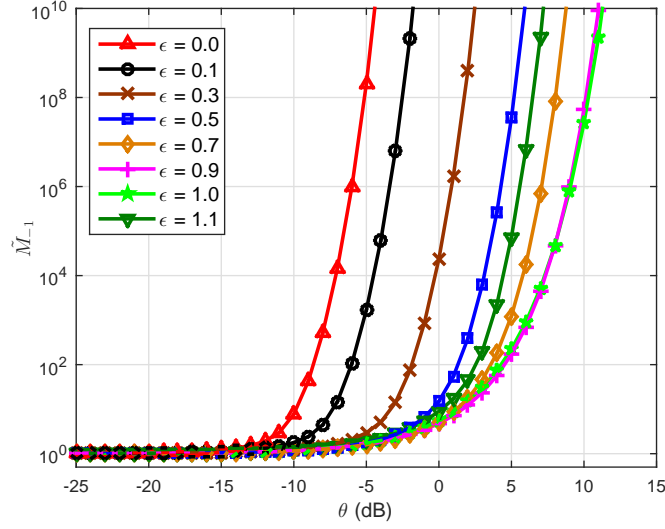


Fig. 8. Analytical results of the mean local delay \tilde{M}_{-1} as a function of θ for different values of ϵ and $\alpha = 3$ in the uplink.

a *phase transition* from finite to infinite when the SIR threshold reaches a critical value. But for uplink Poisson cellular networks with FPC, the curves in Fig. 8 and Fig. 9 show that no phase transition may occur. For a given FPC compensation factor ϵ , the mean local delay stays close to 1 for small and modest values of θ , and quickly increases at higher θ . A higher ϵ is helpful in terms of broadening the SIR range for which the mean local delay is below some threshold. An increase past $\epsilon = 1$, however, is detrimental.

E. Meta distribution: analytical expression, classical bounds

Equipped with a tight approximation for M_b , the analytical meta distribution of the SIR for uplink Poisson cellular networks can be obtained from the Gil-Pelaez theorem [28] as

$$\bar{F}(\theta, x) \approx \frac{1}{2} + \frac{1}{\pi} \int_0^\infty \frac{\Im(e^{-jt \log x} \tilde{M}_{jt})}{t} dt \quad (17)$$

where $\Im(z)$ denotes the imaginary part of the complex number z .

As in [1], some classical bounds can also be directly obtained as follows,

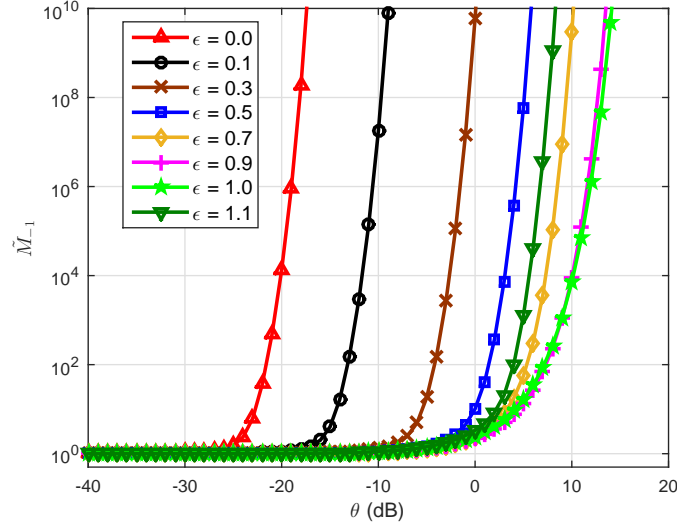


Fig. 9. Analytical results of the mean local delay \tilde{M}_{-1} as a function of θ for different values of ϵ and $\alpha = 4$ in the uplink.

For $x \in [0, 1]$, the Markov bounds of the meta distribution are given by

$$1 - \frac{\mathbb{E}^{!t}((1 - P_s(\theta))^b)}{(1 - x)^b} < \bar{F}(\theta, x) \leq \frac{\tilde{M}_b}{x^b}, \quad b > 0. \quad (18)$$

For $x \in [0, 1]$, let $V \triangleq \text{var } P_s(\theta) = \tilde{M}_2 - \tilde{M}_1^2$, the Chebyshev bounds of the meta distribution are given by

$$\bar{F}_{P_s}(x) > 1 - \frac{V}{(x - \tilde{M}_1)^2}, \quad x < \tilde{M}_1, \quad (19)$$

and

$$\bar{F}_{P_s}(x) > 1 - \frac{V}{(x - \tilde{M}_1)^2}, \quad x > \tilde{M}_1. \quad (20)$$

For $x \in [0, 1]$, let $V \triangleq \text{var } P_s(\theta) = \tilde{M}_2 - \tilde{M}_1^2$, the Paley-Zygmund bound of the meta distribution is given by

$$\bar{F}_{P_s}(x\tilde{M}_1) \geq \frac{(1 - x)^2 \tilde{M}_1^2}{\tilde{M}_2 + x(x - 2)\tilde{M}_1^2}, \quad x \in (0, 1). \quad (21)$$

The Paley-Zygmund bound can be used to roughly quantify the fraction of links that can achieve a certain fraction of the average performance.

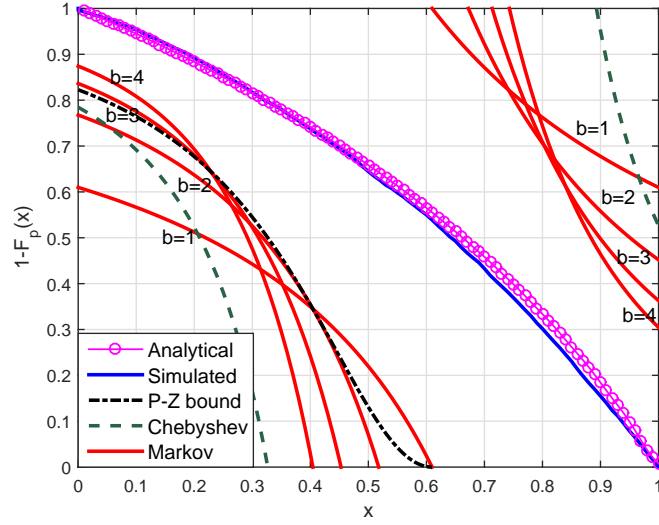


Fig. 10. The analytical meta distribution (17), the Markov bounds (18) for $b \in [4]$, the Chebyshev bounds (19) and (20) and the Paley-Zygmund bound (21) for $\alpha = 4$, $\theta = 0$ dB and $\epsilon = 0.5$ in the uplink.

Fig. 10 shows the meta distribution from both the simulation result and the analytical expression in (17). It proves the correctness of the theoretical analysis. The classical bounds are also illustrated in this figure.

Given the first k moments of $P_s(\theta)$, we can establish the tightest possible lower and upper bounds. Such a problem can be generally formulated as follows. For a random variable Y with the first k moments given by M_1, \dots, M_k , find

$$L(x) \triangleq \min_{F \in \mathcal{M}_k} F(x), \quad x \in (0, 1)$$

and

$$U(x) \triangleq \max_{F \in \mathcal{M}_k} F(x), \quad x \in (0, 1),$$

where \mathcal{M}_k is the class of distributions (cdfs) with the same first k moments as Y .

In our application $Y = P_s(\theta)$, $\mathbb{E}(Y^k) = M_k$, and since we are working with ccdfs, we have

$$1 - U(x) \leq \bar{F}(\theta, x) \leq 1 - L(x).$$

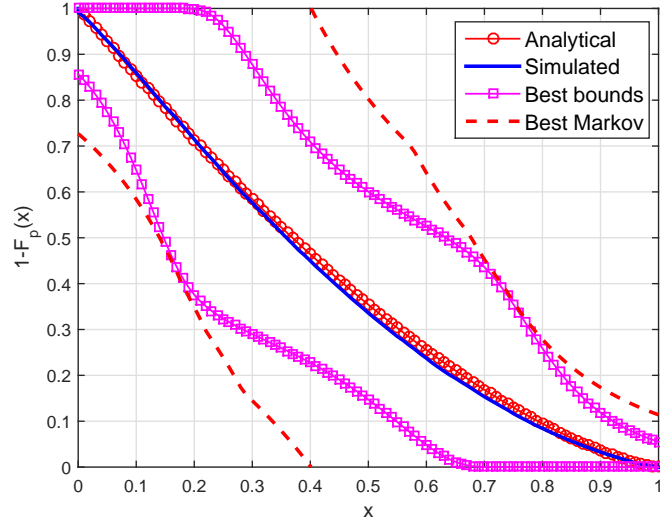


Fig. 11. The meta distribution, the best Markov bounds (18) for $b \in [4]$, and the best bounds (given the first four moments) for $\alpha = 3$, $\theta = 0$ dB and $\epsilon = 0.5$ in the uplink.

The details of the method to determine $L(x)$ and $U(x)$ can be found in [1] and [29]. Fig. 11 shows the best bounds and the lower and upper envelopes of the Markov bounds for $b \in [4]$.

F. Meta distribution: beta distribution approximation

Since $P_s(\theta)$ is supported on $[0, 1]$, it is natural to approximate its distribution with the beta distribution. The pdf of a beta distributed random variable X with mean μ is

$$f_X(x) = \frac{x^{\frac{\mu(\beta+1)-1}{1-\mu}} (1-x)^{\beta-1}}{B(\mu\beta/(1-\mu), \beta)},$$

where $B(\cdot, \cdot)$ is the beta function. The variance is given by

$$\sigma^2 \triangleq \text{var } X = \frac{\mu(1-\mu)^2}{\beta + 1 - \mu}.$$

Matching the mean and variance σ^2 yields $\mu = \tilde{M}_1$ and

$$\beta = \frac{(\mu - \tilde{M}_2)(1 - \mu)}{\tilde{M}_2 - \mu^2}.$$

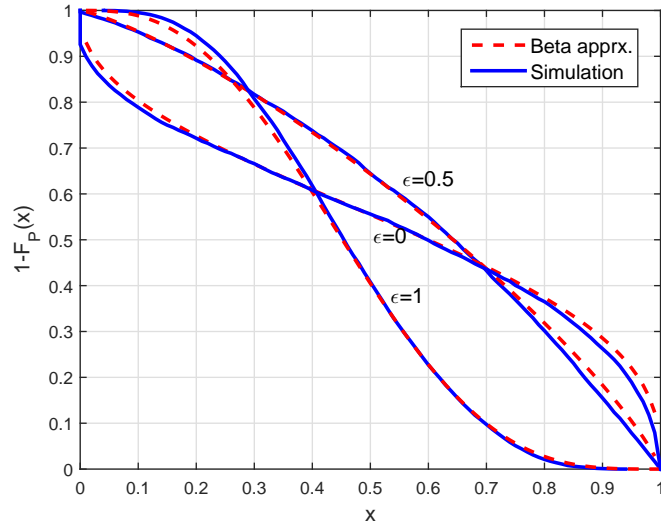


Fig. 12. The meta distribution (simulation result) and the beta distribution approximation for $\alpha = 4$, $\theta = 0$ dB and $\epsilon \in \{0, 0.5, 1\}$ in the uplink.

Fig. 12 shows that the beta distribution is an almost perfect approximation for the meta distribution. The close match between the meta distribution and the beta distribution is very convenient, since it implies that for most purposes, an evaluation of the Gil-Pelaez integral (17) is not needed.

III. META DISTRIBUTION FOR THE DOWNLINK

A. System Model

In this section, we study the fractional power control for downlink cellular networks in the framework of the meta distribution. For the downlink Poisson cellular networks, we follow the usual network model wherein the base stations (BSs) are modeled by a homogeneous PPP $\Phi_b \subset \mathbb{R}^2$ with intensity λ , and we focus on the typical user at the origin, since the downlink receiver is the user. We assume the standard path loss law with the path loss exponent $\alpha > 2$ and power fading coefficients $\{h_x\}$, $x \in \Phi_b$ following exponential distribution with unit mean (*i.e.*, Rayleigh fading) from BS x to the typical user. Denote the link distance from the typical user to its serving BS $x_0 \in \Phi_b$ by R , the distance from the interfering BS x to the typical user

by D_x , and the interfering link distance of BS $x \in \Phi_b \setminus \{x_0\}$ by R_x . Each BS x uses fractional power control $P_x = pR_x^{\alpha\epsilon}$, with p the baseline transmit power and $\epsilon \in [0, 1]$ the compensation parameter. In such a downlink scenario, the interfering BSs strictly form a homogeneous PPP and all of them are further away than the serving BS of the typical user, R_x is independently and identically Rayleigh distributed as R , with pdf $f_R(r) = 2\pi\lambda r \exp(-\lambda\pi r^2)$.

The SIR for the typical user is given by

$$\text{SIR} \triangleq \frac{P_{x_0} h_{x_0} R^{-\alpha}}{\sum_{x \in \Phi_b \setminus \{x_0\}} P_x h_x D_x^{-\alpha}} = \frac{h_{x_0} R^{\alpha(\epsilon-1)}}{\sum_{x \in \Phi_b \setminus \{x_0\}} R_x^{\alpha\epsilon} h_x D_x^{-\alpha}}.$$

B. Moments

Theorem 2 (Moments for downlink Poisson cellular networks) *The b -th moment of the conditional success probability of the downlink Poisson cellular networks with FPC is given by*

$$M_b = \int_0^\infty \exp\left(-z \left(\int_1^\infty f(z, x) dx + 1\right)\right) dz, \quad (22)$$

where $f(z, x) = \int_0^\infty z e^{-zy} \left(1 - \left(1 + \theta y^{\frac{\alpha\epsilon}{2}} x^{-\frac{\alpha}{2}}\right)^{-b}\right) dy$.

Proof: The conditional coverage probability is

$$\begin{aligned} P_s(\theta) &= \mathbb{P}\left(h_{x_0} > \theta \sum_{x \in \Phi_b \setminus \{x_0\}} h_x D_x^{-\alpha} R_x^{\alpha\epsilon} R^{\alpha(1-\epsilon)} \mid \Phi_a, \Phi_b\right) \\ &= \prod_{x \in \Phi_b \setminus \{x_0\}} \frac{1}{1 + \theta \frac{R^{\alpha(1-\epsilon)} R_x^{\alpha\epsilon}}{D_x^\alpha}}. \end{aligned}$$

Then M_b follows as

$$\begin{aligned}
M_b &= \mathbb{E} \prod_{x \in \Phi_b \setminus \{x_0\}} \frac{1}{\left(1 + \theta \frac{R^{\alpha(1-\epsilon)} R_x^{\alpha\epsilon}}{D_x^\alpha}\right)^b} \\
&= \mathbb{E} \prod_{x \in \Phi_b \setminus \{x_0\}} \mathbb{E}_{R_x} \frac{1}{\left(1 + \theta \frac{R^{\alpha(1-\epsilon)} R_x^{\alpha\epsilon}}{D_x^\alpha}\right)^b} \\
&\stackrel{(a)}{=} \mathbb{E} \prod_{x \in \Phi_b \setminus \{x_0\}} \int_0^\infty 2\lambda\pi x e^{-\lambda\pi x^2} \frac{1}{\left(1 + \theta x^{\alpha\epsilon} D_x^{-\alpha} R^{\alpha(1-\epsilon)}\right)^b} dx \\
&\stackrel{(b)}{=} \mathbb{E}_R \int_R^\infty -2\lambda\pi \left(1 - \int_0^\infty 2\lambda\pi x e^{-\lambda\pi x^2} \frac{1}{\left(1 + \theta x^{\alpha\epsilon} a^{-\alpha} R^{\alpha(1-\epsilon)}\right)^b} dx\right) da, \quad (23)
\end{aligned}$$

where (a) is due to R_x following the Rayleigh distribution; (b) follows from the PGFL of the homogeneous PPP [2] and the fact that D_x is strictly greater than R . M_b is then obtained by averaging over R as

$$M_b = \int_0^\infty 2\lambda\pi r \exp\left(\int_r^\infty -2\lambda\pi a \left(1 - \int_0^\infty 2\lambda\pi x e^{-\lambda\pi x^2} \frac{1}{\left(1 + \theta x^{\alpha\epsilon} a^{-\alpha} r^{\alpha(1-\epsilon)}\right)^b} dx\right) da\right) e^{-\lambda\pi r^2} dr. \quad (24)$$

Then using substitution $\frac{x}{r} = u$, $\frac{r}{a} = v$ and $e^{-\lambda\pi r^2} = t$, after some simplification, we get the final result in (22). ■

Note that in contrast to the uplink case, (22) is an exact expression.

Fig. 13 shows the downlink standard success probability $M_1 = p_s$ and the variance of the conditional success probability as a function of θ for $\alpha = 4$ and FPC parameter $\epsilon = 0, 0.5, 1$. The solid and dashed curves correspond to the simulation result, and the markers correspond to the analytical result by Theorem 2. These results show that the analytical results closely match the simulation results and also reveal that an appropriate FPC parameter can help mitigate the variance while maintaining the level of M_1 , at least for a certain SIR range. For example, for $\epsilon = 0.5$ and an SIR range from -10 dB to 5 dB, M_1 stays at almost the same level, but the variance is significantly reduced compared to the case without power control. Hence, by studying power control with the tool of meta distribution, we find that FPC can bring some fairness benefits to the downlink.

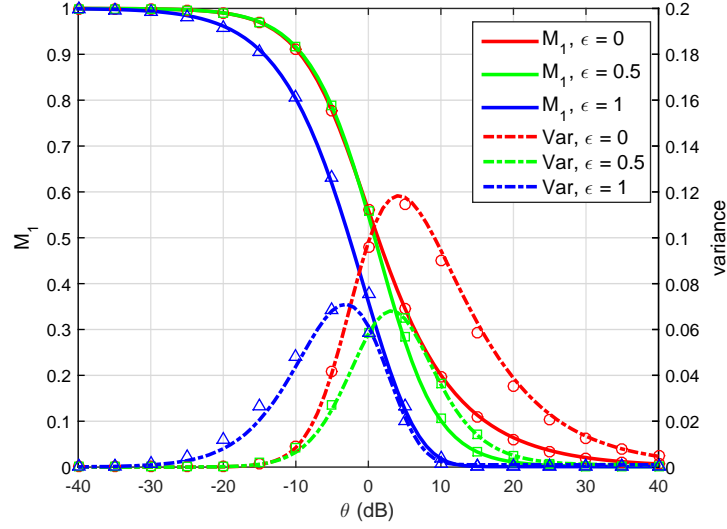


Fig. 13. Downlink M_1 and variance of $P_s(\theta)$ obtained from simulation and analysis for different ϵ and $\alpha = 4$. The curves are the analytical results from Theorem 2 and the markers correspond to the simulation results.

Remark 3: For the case without power control, *i.e.*, $\epsilon = 0$, the b -th moment of the conditional success probability for Poisson cellular network downlinks has a closed-form expression, given in [1, Eqn. (21)], namely

$$M_b = \frac{1}{{}_2F_1(b, -\delta; 1 - \delta; -\theta)}, \quad b \in \mathbb{C}. \quad (25)$$

Based on Theorem 2, we have the following statements for the downlink mean local delay.

Corollary 3 (Mean local delay for downlink Poisson cellular networks) *When $\alpha > 2$, the downlink mean local delay for Poisson cellular networks with FPC is given by,*

$$M_{-1} = \int_0^\infty \exp(c\Gamma(1 + \rho)y^{1-\rho} - y)dy, \quad (26)$$

where $c = \theta\delta/(1 - \delta)$, $\rho = \epsilon/\delta$ and $\delta = 2/\alpha$.

Proof: By substituting $b = -1$ in (22), we obtain M_{-1} in the form

$$\begin{aligned} M_{-1} &= \int_0^\infty \exp \left(\theta z^2 \int_1^\infty \int_0^\infty e^{-zy} y^{\alpha\epsilon/2} x^{-\alpha/2} dy dx - z \right) dz \\ &= \int_0^\infty \exp \left(\theta \int_1^\infty x^{-\alpha/2} dx \int_0^\infty z^2 e^{-zy} y^{\alpha\epsilon/2} dy - z \right) dz, \end{aligned}$$

by noticing that $\int_1^\infty x^{-\alpha/2} dx = \frac{1}{-1+\alpha/2}$ and $\int_0^\infty z^2 e^{-zy} y^{\alpha\epsilon/2} dy = z^{1-\epsilon\alpha/2} \Gamma(1 + \epsilon\alpha/2)$, after the substitution, we get the final expression in (26). ■

Corollary 4 (Convergence of the downlink mean local delay) *When $\alpha > 2$, M_{-1} is finite for any θ if $0 < \epsilon \leq \delta$; for $\epsilon = 0$, M_{-1} is finite if $\theta < 1/\delta - 1$; if $\epsilon > \delta$, then M_{-1} is ∞ for all θ .*

Proof: In (26), since $\delta < 1$, we have $c > 0$ and $1 - \rho \leq 1$. To make M_{-1} finite, $1 - \rho$ must be non-negative. Thus we have $0 \leq 1 - \epsilon/\delta \leq 1$, which gives us $0 \leq \epsilon \leq \delta$. Moreover, when $\epsilon = 0$, then $\rho = 0$, c must be smaller than 1 to guarantee the convergence of the integral. ■

Remark 4: Cor. 4 indicates that the phase transition of the mean local delay in downlink Poisson cellular networks only occurs at $\epsilon = 0$, *i.e.*, when there is no power control. The mean local delay for $\epsilon = 0$ has been derived in [1] and is given by

$$M_{-1} = \frac{1 - \delta}{1 - \delta(1 + \theta)} = \frac{1}{1 - \frac{\delta}{1-\delta}\theta}, \quad \theta < 1/\delta - 1. \quad (27)$$

The critical SIR threshold is $\theta_c = 1/\delta - 1$.

Remark 5: For $\epsilon = \delta/2$ and $\epsilon = \delta$, M_{-1} also has closed-form expressions, given by (28) and (29), respectively.

$$\epsilon = \frac{\delta}{2} : \quad M_{-1} = 1 + \frac{\theta}{2} \cdot \frac{\delta}{1-\delta} \sqrt{\pi} \exp \left(\frac{\theta^2}{4} \cdot \left(\frac{\delta}{1-\delta} \right)^2 \right) \operatorname{erfc} \left(-\frac{\theta}{2} \cdot \frac{\delta}{1-\delta} \right) \quad (28)$$

$$\epsilon = \delta : \quad M_{-1} = \exp \left(\frac{\delta}{1-\delta} \theta \right) \quad (29)$$

Interestingly, $\frac{\delta}{1-\delta}$ is exactly the mean interference-to-signal ratio (MISR) of the PPP introduced in [30], hence, (27), (28) and (29) can also be expressed as a function of the MISR.

Fig. 14 and Fig. 15 show the analytical results of M_{-1} for different ϵ . It can be seen that for large θ , $\epsilon = \delta$ is optimal for the minimization of the mean local delay, while for small θ , $\epsilon = \delta/2$

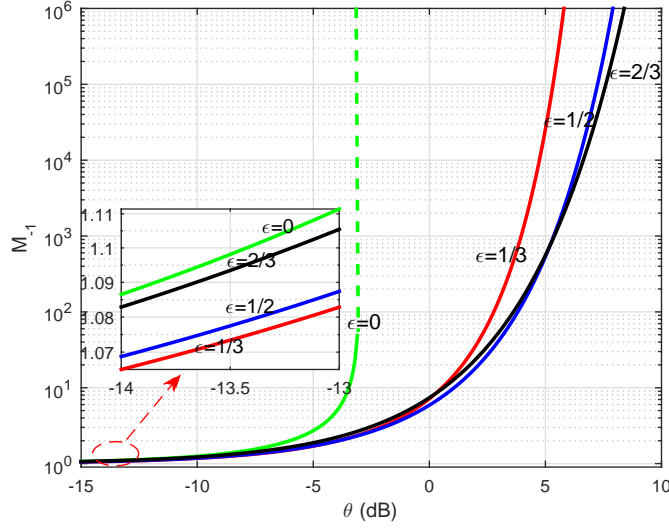


Fig. 14. Downlink mean local delay as a function of θ obtained from analytical results for $\alpha = 3$ and different ϵ , where $\epsilon = 0$ corresponds to (27), $\epsilon = 1/3$ corresponds to (28) and $\epsilon = 2/3$ corresponds to (29). A phase transition occurs at $\theta = -3$ dB when $\epsilon = 0$.

is the optimal to minimize the mean local delay.

Remark 6: Letting $\rho_{\text{opt}}(c) = \arg \min_{\rho} M_{-1}$, a detailed numerical study of (26) shows that $\lim_{c \rightarrow 0} \rho_{\text{opt}} = 1/2$ and $\lim_{c \rightarrow \infty} \rho_{\text{opt}} = 1$. A small c can be achieved by either a small θ or a small δ , while a large c can be achieved by either a large θ or a δ close to 1.

C. Meta Distribution: exact expression, bounds and beta approximation

Following the same methods used in the uplink analysis, the exact downlink meta distribution for Poisson cellular networks can be calculated by using the Gil-Pelaez theorem, the classical bounds and the best bounds for the downlink meta distribution are also obtained and shown in Fig. 16 and Fig. 17. The beta approximation of the meta distribution by matching the mean and variance is shown in Fig. 18.

IV. CONCLUSIONS

This paper applies the concept of the meta distribution, which is the distribution of the conditional success probability, to study the uplink and downlink scenarios in Poisson cellular

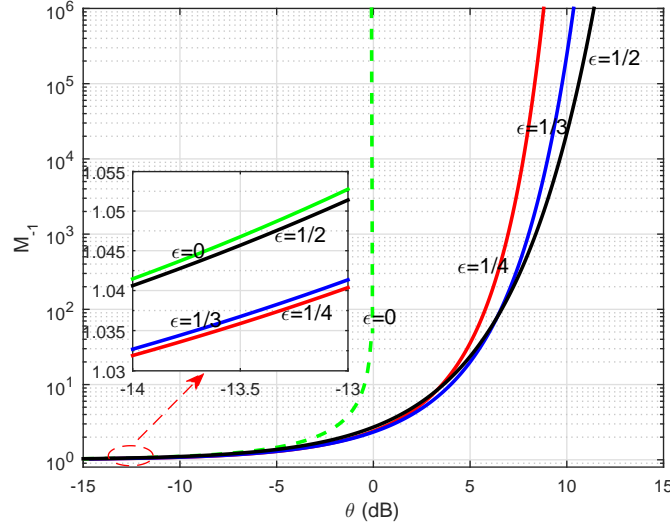


Fig. 15. Downlink mean local delay as a function of θ obtained from analytical results for $\alpha = 4$ and different ϵ , where $\epsilon = 0$ corresponds to (27), $\epsilon = 1/4$ corresponds to (28) and $\epsilon = 1/2$ corresponds to (29). A phase transition occurs at $\theta = 0$ dB when $\epsilon = 0$.

networks with fractional power control. For the uplink scenario, the interfering user point process relative to the typical BS is approximated to a non-homogeneous PPP which is developed by analyzing the pair correlation function of the interfering points. This approximation yields analytical results that are highly consistent with the simulation results. For both scenarios, the general expression of the moments, the analytical results for the mean local delay and the analytical expression for the distribution of the conditional success probability are provided, revealing much more detailed information about the user performance in the cellular networks than just the standard success probability M_1 . Moreover, it is shown that both the uplink and downlink meta distributions can be closely approximated by the beta distribution through matching the mean and variance, which is convenient for the network performance analysis with no need for calculating higher-order moments.

The study of the mean local delay does not indicate any phase transition in the uplink. For the downlink, the phase transition only occurs when there is no power control. The optimum power control parameter that minimizes the mean local delay in the downlink is between $\delta/2$ and δ .

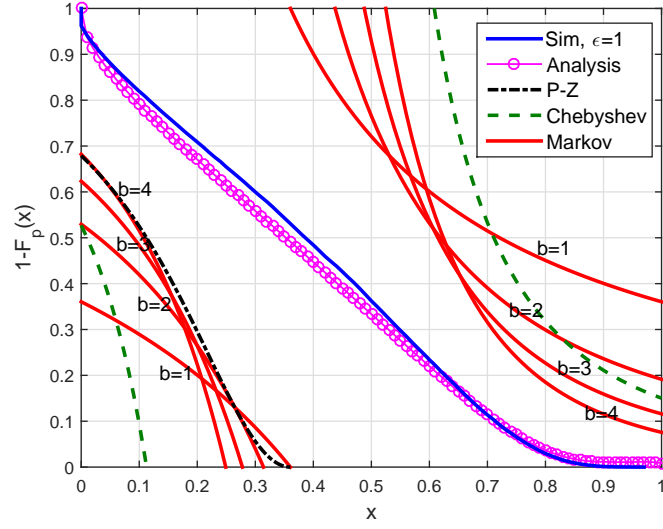


Fig. 16. The exact meta distribution (17), the Markov bounds (18) for $b \in [4]$, the Chebyshev bounds (19) and (20) and the Paley-Zygmund bound (21) for $\alpha = 4$, $\theta = 0$ dB and $\epsilon = 1$ in downlink Poisson cellular networks.

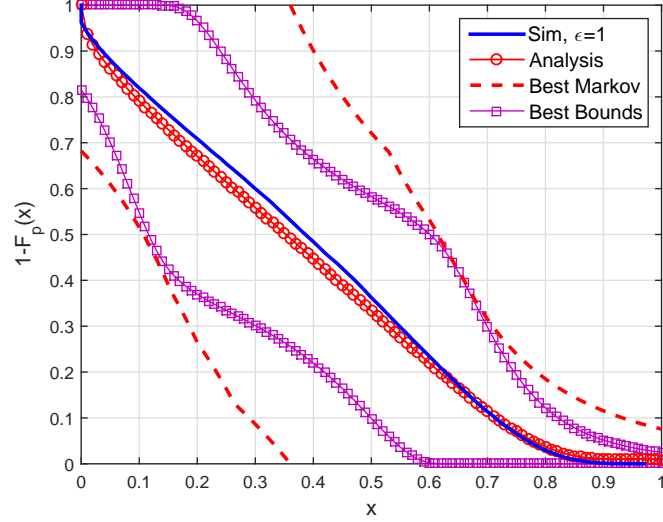


Fig. 17. Both the simulated and the exact meta distribution (17), the best Markov bounds (18) for $b \in [4]$, and the best bounds (given the first four moments) for $\alpha = 4$, $\theta = 0$ dB and $\epsilon = 1$ in downlink Poisson cellular networks.

The investigation of the fractional power control in both the uplink and downlink shows that compensating the path loss sensibly benefits the user fairness while maintaining the average overall network performance. It also reveals that the effect of FPC is mainly a *concentration*

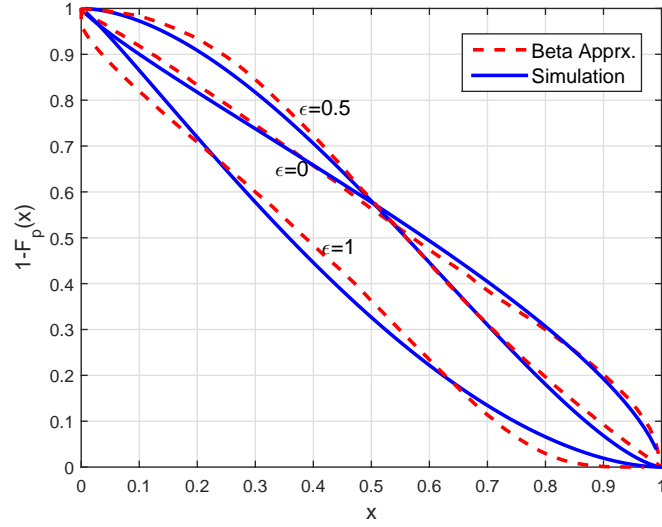


Fig. 18. The meta distribution (simulation result) and the beta distribution approximation for $\alpha = 4$, $\theta = 0$ dB and $\epsilon \in \{0, 0.5, 1\}$ in the downlink.

in the user performance levels, which means M_1 alone does not give enough information about what parameter to use, but by virtue of the meta distribution, we can obtain more fine-grained information (e.g., the variance) to find the best ϵ . Such advantages of the meta distribution are helpful to the operators in practical network deployment and configuration.

REFERENCES

- [1] M. Haenggi, “The meta distribution of the SIR in Poisson bipolar and cellular networks,” *IEEE Trans. Wireless Commun.*, vol. 15, no. 44, pp. 2577–2589, Apr. 2016.
- [2] M. Haenggi, *Stochastic Geometry for Wireless Networks*. Cambridge University Press, 2012.
- [3] F. Baccelli and B. Blaszczyszyn, “A new phase transitions for local delays in MANETs,” in *Proc. IEEE INFOCOM’10*, San Diego, CA, USA, Mar. 2010, pp. 1–9.
- [4] R. K. Ganti and J. G. Andrews, “Correlation of link outages in low-mobility spatial wireless networks,” in *Proc. 44th Asilomar Conf. Signals Syst. Comput. (Asilomar’10)*, Pacific Grove, CA, USA, Nov. 2010, pp. 312–316.
- [5] M. Salehi, A. Mohammadi, and M. Haenggi, “Analysis of D2D underlaid cellular networks: SIR meta distribution and mean local delay,” Submitted. Available at <https://www3.nd.edu/~mhaenggi/pubs/tcom17b.pdf>.
- [6] J. G. Andrews, F. Baccelli, and R. K. Ganti, “A tractable approach to coverage and rate in cellular networks,” *IEEE Trans. Commun.*, vol. 59, no. 11, pp. 3122–3134, Oct. 2011.
- [7] B. Blaszczyszyn, M. K. Karray, and H. P. Keeler, “Using Poisson processes to model lattice cellular networks,” in *Proc. IEEE INFOCOM’13*, Turin, Italy, Apr. 2013, pp. 773–781.

- [8] H. ElSawy, E. Hossain, and M. Haenggi, "Stochastic geometry for modeling, analysis, and design of multi-tier and cognitive cellular wireless networks: A survey," *IEEE Commun. Surveys Tuts.*, vol. 15, no. 3, pp. 996–1019, Jun. 2013.
- [9] W. Lu and M. Di Renzo, "Stochastic geometry modeling of cellular networks: analysis, simulation and experimental validation," in *Proc. ACM Int. Conf. Modeling, Anal. Simul. Wireless Mobile Syst.*, 2015, pp. 179–188.
- [10] X. Zhang and M. Haenggi, "A stochastic geometry analysis of inter-cell interference coordination and intra-cell diversity," *IEEE Trans. Wireless Commun.*, vol. 13, no. 12, pp. 6655–6669, Dec. 2014.
- [11] G. Nigam, P. Minero, and M. Haenggi, "Coordinated multipoint joint transmission in heterogeneous networks," *IEEE Trans. Commun.*, vol. 62, no. 11, pp. 4134–4146, Oct. 2014.
- [12] G. Nigam, P. Minero, and M. Haenggi, "Spatiotemporal cooperation in heterogeneous cellular networks," *IEEE J. Sel. Areas Commun.*, vol. 33, no. 6, pp. 1253–1265, Mar. 2015.
- [13] A. Rajanna and M. Haenggi, "Downlink coordinated joint transmission for mutual information accumulation," Submitted. Available at <http://www3.nd.edu/~mhaenggi/pubs/tcom16c.pdf>.
- [14] H. S. Dhillon, M. Kountouris, and J. G. Andrews, "Downlink MIMO HetNets: modeling, ordering results and performance analysis," *IEEE Trans. Wireless Commun.*, vol. 12, no. 10, pp. 5208–5222, Sep. 2013.
- [15] E. Björnson, L. Sanguinetti and M. Kountouris, "Deploying dense networks for maximal energy efficiency: small cells meet massive MIMO," *IEEE J. Sel. Areas Commun.*, vol. 34, no. 4, pp. 832–847, Sep. 2016.
- [16] G. George, R. K. Mungara, A. Lozano, and M. Haenggi, "Ergodic spectral efficiency in MIMO cellular networks," *IEEE Trans. Wireless Commun.*, accepted. Available at <https://arxiv.org/pdf/1607.04352v2.pdf>.
- [17] H. Sun, M. Wildemeersch, M. Sheng, and T. Q. Quek, "D2D enhanced heterogeneous cellular networks with dynamic TDD," *IEEE Trans. Wireless Commun.*, vol. 14, no. 8, pp. 4204–4218, Mar. 2015.
- [18] J. Liu, S. Zhang, H. Nishiyama, N. Kato, and J. Guo, "A stochastic geometry analysis of D2D overlaying multi-channel downlink cellular networks," in *Proc. IEEE INFOCOM'15*, Hong Kong, Apr. 2015, pp. 46–54.
- [19] Q. Ye, M. Al-Shalash, C. Caramanis, and J. G. Andrews, "A tractable model for optimizing device-to-device communications in downlink cellular networks," in *Proc. IEEE ICC'14*, Sydney, Australia, Jun. 2014, pp. 2039–2044.
- [20] H. ElSawy and E. Hossain, "On stochastic geometry modeling of cellular uplink transmission with truncated channel inversion power control," *IEEE Trans. Wireless Commun.*, vol. 13, no. 8, pp. 4454–4469, Apr. 2014.
- [21] H. Y. Lee, Y. J. Sang, and K. S. Kim, "On the uplink SIR distributions in heterogeneous cellular networks," *IEEE Commun. Lett.*, vol. 18, no. 12, pp. 2145–2148, Oct. 2014.
- [22] S. Singh, X. Zhang, and J. G. Andrews, "Joint rate and SINR coverage analysis for decoupled uplink-downlink biased cell associations in HetNets," *IEEE Trans. Wireless Commun.*, vol. 14, no. 10, pp. 5360–5373, Oct. 2015.
- [23] J. G. Andrews, A. K. Gupta, and H. S. Dhillon, "A primer on cellular network analysis using stochastic geometry," *arXiv preprint arXiv:1604.03183*, Apr. 2016.
- [24] P. Calka and T. Schreiber, "Limit theorems for the typical Poisson-Voronoi cell and the Crofton cell with a large inradius," *Annals of Probability*, vol. 33, pp. 1625–1642, Jul. 2005.
- [25] T. Bai and R. W. Heath, "Analyzing uplink SINR and rate in massive MIMO systems using stochastic geometry," *IEEE Trans. Commun.*, vol. 64, no. 11, pp. 4592–4606, Jul. 2016.
- [26] M. Haenggi, "User point processes in cellular networks," *arXiv preprint arXiv:1611.08560*, Nov. 2016.

- [27] M. Haenggi, "The local delay in Poisson networks," *IEEE Trans. Inf. Theory*, vol. 59, pp. 1788–1802, Mar. 2013.
- [28] J. Gil-Pelaez, "Note on the inversion theorem," *Biometrika*, vol. 38, no. 3-4, pp. 481–482, 1951.
- [29] S. Rácz, Á. Tari, and M. Telek, "A moments based distribution bounding method," *Mathematical and computer modelling*, vol. 43, no. 11, pp. 1367–1382, 2006.
- [30] M. Haenggi, "The mean interference-to-signal ratio and its key role in cellular and amorphous networks," *IEEE Wireless Communications Letters*, vol. 3, pp. 597–600, Dec. 2014.